American Journal of Science and Technology
2017; 4(3): 28-42
http://www.aascit.org/journal/ajst
ISSN: 2375-3846

AASCIT American Association for Science and Technology

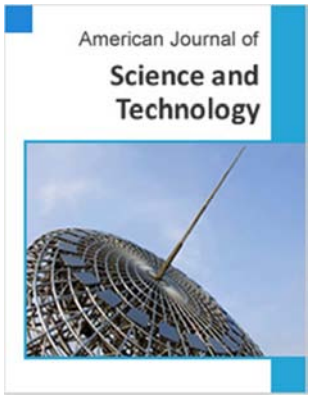

Keywords
FACTS,
Wind Power,
Electromechanical Oscillations,
POD Design,
Modal Analysis,
Time Domain Simulation,
Control Design

Received: March 30, 2017
Accepted: April 18, 2017
Published: June 9, 2017

FACTS-Based Stabilization of the Dynamic Stability of Weakly Interconnected Systems Considering Wind Power Integration

Mohamed EL-Shimy Mahmoud Bekhet[1, *], Fahmy Metwali Ahmed Bendary[2], Wagdy Mohamed Mansour[2], Mohamed Adel Mandour[2]

[1]Faculty of Engineering, Electric Power and Machines Department, Ain Shams University, Cairo, Egypt
[2]Faculty of Engineering, Electric Power and Machines Department, Benha University, Cairo, Egypt

Email address
ShimyMB@yahoo.com (M. EL-Shimy M. B.),
mohamed_bekhet@eng.asu.edu.eg (M. EL-Shimy M. B.)
[*]Corresponding author

Citation
Mohamed EL-Shimy Mahmoud Bekhet, Fahmy Metwali Ahmed Bendary, Wagdy Mohamed Mansour, Mohamed Adel Mandour. FACTS-Based Stabilization of the Dynamic Stability of Weakly Interconnected Systems Considering Wind Power Integration. *American Journal of Science and Technology*. Vol. 4, No. 3, 2017, pp. 28-42.

Abstract
This paper presents an analysis of the dynamic stability of weakly interconnected power systems considering the impacts of wind power technologies and FACTS devices. In addition, the paper presents the design and verification of FACTS-based supplementary controls for power oscillation damping (POD). Both the traditional frequency domain and adaptive genetic algorithm (GA) based designs of POD controllers are presented. Due to their variable and intermittent nature, large changes in the power production from wind farms are usually detected. Therefore, the effectiveness of the traditional POD controller design is investigated considering a wide range of operating conditions. The integration of wind power in power systems is considered from two perspectives; replacement and addition. In the replacement situation, a specific amount of conventional power is replaced with the same amount of wind power. On the other hand, the addition situation refers to adding wind power to an existing conventional power generation system. The study system is composed of two weakly interconnected areas. The objectives of wind power integration are to reduce the dependency between the two areas and to reduce the use of the conventional fuels. The integration process is subjected to the minimum damping constraint for keeping system dynamic stability. Two popular wind energy technologies are considered which are fixed speed SCIGs and the variable speed DFIGs. The results show that the wind power causes reduction in the damping of power system oscillations. Therefore, POD controllers are integrated with the available SVCs to improve the system dynamic stability. The POD designs are evaluated by the modal analysis and the time-domain simulation.

1. Introduction

Since the early till the present power systems, the power system stability problem has been given a high attention for secure operation, and planning of power systems.

Regardless of the size and structure of a power system, the stability is a major challenge; however, recent power systems are more susceptible to instabilities due to the present of new power generation and network control technologies [1 - 3]. The penetration level ofrenewable energy technologies - such as wind and solar sources – in power systems are recently increasing with an increasing trend. This is due to their ecological benefits and the shortage of conventional fuels [4].

Despite its benefits, wind and solar sources are operationally characterized by high variability and intermittency. This situation results in a significant reduction in the predictability of the power generation from these sources in comparison with conventional sources [5 – 8]. Consequently, sudden unexpected changes in the power production from variable renewable sources are probable. This significantly upsets the stability and security of power systems; however, the impact of variable energy sources on the stability of power systems is highly related to their penetration level; the impact increases with the increase in the penetration level [4, 10, 11].

From network point of view, recent group of technologies are created for rapidly controlling and enhancing the performance as well as the security of power systems. These technologies are called FACTS devices. According to [9], the FACTS devices are defined as "power electronic based controllers and other static equipment which can regulate the power flow and transmission voltage through rapid control action". Unless they are equipped with proper supplementary controls, some of the FATCS devices show adverse impacts on the damping of power system oscillations. These supplementary controls are very similar to the traditional power systems stabilizers (PSSs) of conventional synchronous generators and they are called power oscillation damping (POD) controllers [2, 3, 10 – 13].

The tuning of POD parameters can be obtained through traditional control design or artificial intelligence (AI) techniques. The most common traditional techniques are based on the frequency response [14], pole placement [15], eigenvalues sensitivity [15] and residue method [10]; however the AI techniques are based on fuzzy control, neural networks, and genetic algorithms [16]. The handling of system nonlinearities is the main advantage of the AI design techniques over the traditional design techniques. In addition, the AI based techniques can be easily fit to the adaptive control design requirements.

This paper extends the POD traditional design techniques presented in [11, 20, 21] by considering the GA optimization based technique for adaptive POD design. Popular wind energy technologies (fixed speed SCIG and variable speed DFIG) [6, 25] are considered while two integration scenarios are analysed. In the power replacement scenario, a specific amount of conventional power is replaced by wind power while the wind power is added to the system in the power addition scenario. The overall conventional fuel consumption is reduced as an outcome of both integration scenarios. On the other hand, the power addition is used, in this paper, to reduce the power transfer dependency between weakly interconnected areas. In both integration scenarios, the maximum penetration level of wind power integration is determined based on the dynamic stability of power systems through the modal analysis. The POD design is then performed for realizing an acceptable damping level of the system. A damping ratio between 5% and 10% is acceptable for most power utilities; however, a minimum damping ratio of 10% is recommended for secure system operation [11, 21]. The MATLAB control and GA toolboxes [25] are used in the POD design while the eigenvalue analysis and the time-domain simulations are performed using the PSAT toolbox version 2.1.7 [23, 24].

2. Dynamic Modeling and POD Tuning

This section presents the linearized modeling of power systems for modal analysis and POD design. In this paper, the POD is designed as a supplementary control for static VAr compensators (SVCs). The SVCs are a category of shunt-connected FACTS devices used mainly for bus voltage control. Generalized modeling of FACTS devices is presented in [1] while a simplified model for the SVC is presented in this section. The model of the POD is also included.

2.1. Linearized Modeling and Modal Analysis

Power systems are dynamic systems that can be represented by differential algebraic equations in combination with non-linear algebraic equations. Hence, a power system can be dynamically described by a set of n first order nonlinear ordinary differential equations. These equations are to be solved simultaneously. In vector-matrix notation, these equations are expressed as,

$$\dot{x} = f(x,u) \tag{1}$$

$$y = g(x,u) \tag{2}$$

where: $x = [x_1, x_2 \cdots x_n]^{\mathrm{t}}$, $u = [u_1, u_2 \cdots u_n]^t$, $f = [f_1, f_2 \cdots f_n]^t$, $y = [y_1, y_2 \cdots y_n]^t$, $g = [g_1, g_2 \cdots g_n]^t$, n is the order of the system, r is the number of inputs, and m is the number of outputs.

The column vector x is called the state vector and its entries are the state variables. The vector u is the vector of inputs to the system, which are external signals that have an impact on the performance of the system. The output variables (y) are those that can be observed in the system. The column vector y is the vector of system output variables, referred as output vector and g is the vector of nonlinear functions defining the output variables in terms of state and input variables.

The design of POD controllers is based on a linearized model of the system. After solving the power flow problem, a modal analysis is carried out by computing the eigenvalues and the participation factors of the state matrix of the system. The dynamic system is put into state space form as a combination of coupled first order, linearized differential

equations that take the form,

$$\Delta\dot{x} = A\Delta x + B\Delta u \quad (3)$$

$$y = C\Delta x + D\Delta u \quad (4)$$

where Δ represents a small deviation, A is the state matrix of size $n \times n$, B is the control matrix of size $n \times r$, C is the output matrix of size $m \times n$, and D is the feed forward matrix of size $m \times r$. The values of the matrix D define the proportion of input which appears directly in the output.

The eigenvalues λ of the state matrix A can be determined by solving $\det[A - \lambda I] = 0$. Let the i^{th} eigenvalue of the state matrix A takes the form $\lambda_i = \sigma_i \pm j\omega_i$; the real part gives the damping, and the imaginary part gives the frequency of oscillation. The relative damping ratio is then given by:

$$\xi_i = -\sigma_i / \sqrt{\sigma_i^2 + \omega_i^2} \quad (5)$$

If the state space matrix A has n distinct eigenvalues, then the diagonal matrix of the eigenvalues (Λ), the right eigenvectors (Φ), and the left eigenvectors (Ψ) are related by the following equations.

$$A\Phi = \Phi\Lambda \quad (6)$$

$$\Psi A = \Lambda\Psi \quad (7)$$

$$\Psi = \Phi^{-1} \quad (8)$$

In order to modify a mode of oscillation by a feedback controller, the chosen input must excite the mode and it must also be visible in the chosen output. The measures of those two properties are the controllability and observability, respectively. The modal controllability ($\acute{B}$) and modal observability ($\acute{C}$) matrices are respectively defined by,

$$\acute{B} = \Phi^{-1}B \quad (9)$$

$$\acute{C} = C\Phi \quad (10)$$

The mode is uncontrollable if the corresponding row of the matrix $\acute{B}$ is zero. The mode is unobservable if the corresponding column of the matrix $\acute{C}$ is zero. If a mode is neither controllable nor observable, the feedback between the output and the input will have no effect on the mode.

2.2. SVC and POD Modeling

In this paper, a simplified time constant regulator is used to represent the SVC (Figure 1). This model is widely used in stability analysis of power systems. As shown, the regulator has an anti-windup limiter. Therefore, the reactance b_{SVC} is locked if one of its limits is reached and the first derivative is set to zero. In this model, a the dynamics of the SVC takes the form,

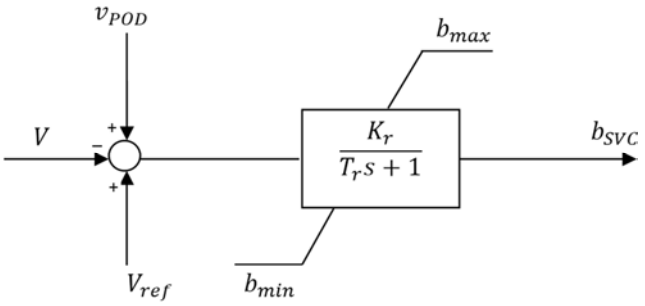

Figure 1. *Simplified time-constant regulator model of SVCs.*

$$\dot{b}_{SVC} = \left(K_r(v_{ref} + v_{POD} - v) - b_{SVC}\right) / T_r \quad (11)$$

The model is completed by the algebraic equation expressing the reactive power injected at the SVC node (Q_{SVC}),

$$Q_{SVC} = b_{SVC}V^2 \quad (12)$$

The structure of the POD controller (Figure 2) is similar to the structure of the classical power system stabilizer (PSS). The controller consists of a stabilizer gain, a washout filter, and phase compensator blocks. The washout signal ensures that the POD output is zero in steady-state. The output signal v_{POD} is subjected to an anti-windup limiter and its dynamics are dependent on a small time constant T_r (in this analysis T_r = 0.01 s). The gain K_w determines the amount of damping introduced by the POD and the phase compensator blocks provide the appropriate phase lead-lag compensation of the input signal (v_{si}). The input signal is selected based on the effectiveness of various observable and controllable inputs signals for power oscillation damping. The input signal may include, but not limited to, line current flow, line active power flow, line reactive power flow, and bus voltage. In this layout, T_3 and T_4 are usually taken equal to T_1 and T_2 respectively.

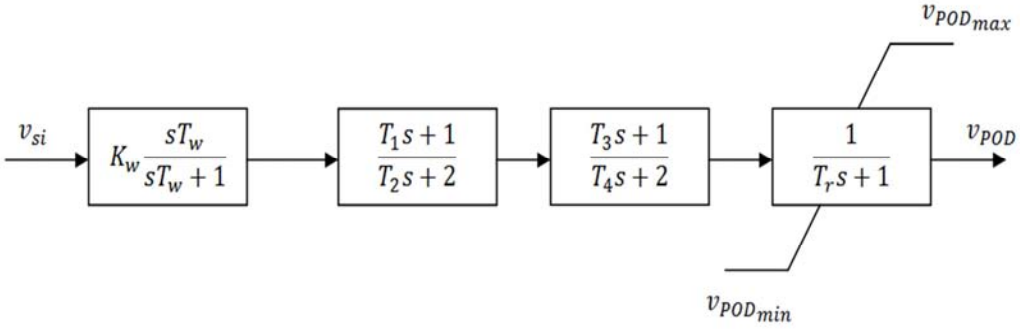

Figure 2. *Scheme of the POD controller.*

2.3. POD Tuning

In this paper two approaches of the tuning of POD parameters are considered. The first approach is the traditional frequency response method while the second approach is based on the GA optimization. Details of the frequency response based POD design are available in [11, 20, 21] while the proposed GA optimization based POD design in briefly described in this section.

The GA is successfully applied to many engineering and optimization problems [17]. It is a powerful domain independent search technique inspired by Darwinian Theory of evolution and it was invented by John Holland and his colleagues in 1970s. The GA is an adaptive learning heuristic technique that imitates the natural process of evolution to progress toward the optimum by performing an efficient and systematic search of the solution space. A set of solutions, described as a population of individuals, are encoded as binary strings, termed as chromosomes. This population represents points in the solution space. A new set of solutions, called off-springs, are created in a new generation (iteration) by crossing some of the strings of the current generation. This process is called crossover. Furthermore, the crossover is repeated at every generation and new characteristics are introduced to add diversity. The process of altering some of the strings of the off-springs randomly is known as mutation. The GA processes are illustrated in the flowchart of Figure 3.

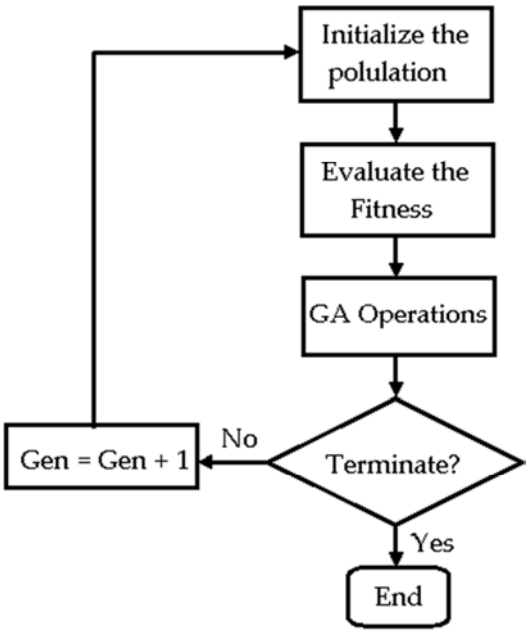

Figure 3. *Basic functions of GA.*

As described by equation (13), the POD design problem is formulated as a constrained optimization problem where the minimization of the integral square error (*ISE*) is the objective function and the minimum damping ratio of any eigenvalue are the constraints.

$$\left.\begin{array}{c} \min ISE = \int_0^{t_s} \Delta\delta^2 \, dt \\ s.t \\ \xi_i \geq 10\%; i = 1 \ldots N \end{array}\right\} \quad (13)$$

where t_s is the simulation time, $\Delta\delta$ is the difference between the machine angle and its reference value, and N is the number of eigenvalues of the system. The reference value of the machine angle is determined from the pre-fault load flow analysis while the machine angle is its instantaneous values caused by the disturbance. The GA optimization is performed using the MATLAB *GA toolbox*. A script file is created to link the PSAT model with the GA toolbox for achieving the optimization problem described by equation (13). Consequently, the POD parameters (K_w, T_1 and T_2) are determined. These three variables are the output of the design steps and their values guarantee the satisfaction of the optimization problem.

3. The Study System and Study Scenarios

The study system is shown in Figure 4. The system data are available at [18]. Each area consists of two synchronous generator units. The rating of each synchronous generator is 900 MVA and 20 kV. Each of the units is connected through transformers to the 230 kV transmission line. There is a power transfer of 400 MW from Area 1 to Area 2. The detailed base data, the line data, and the dynamic parameters for the machines, AVRs, PSS, and loads are given in [18]. This system will be studied and analyzed with the aid of the Power System Analysis Toolbox (PSAT) version 2.1.7 and the control system toolbox of MATLAB 2012a [23-25]. The original Kundur two-area system (Figure 4(a)) has been taken from [18] and has been modified by replacing the old fixed capacitors at buses 7 and 9 by SVCs as shown in Figure 4(b). The wind power integration at bus k of the study system is illustrated at Figure 4(c) where k is either bus 6 or bus 10. The PSAT model of the system shown in Figure 4(b) is shown in Figure 5.

The wind power is included in the system considering two scenarios where two situations are considered in each scenario. A scenario is associated with the WTG technology while a situation is associated with the way at which the wind power is included. The first scenario considers the fixed-speed SCIG while the second one considers the variable-speed DFIGURE For both scenarios the following situations are considered.

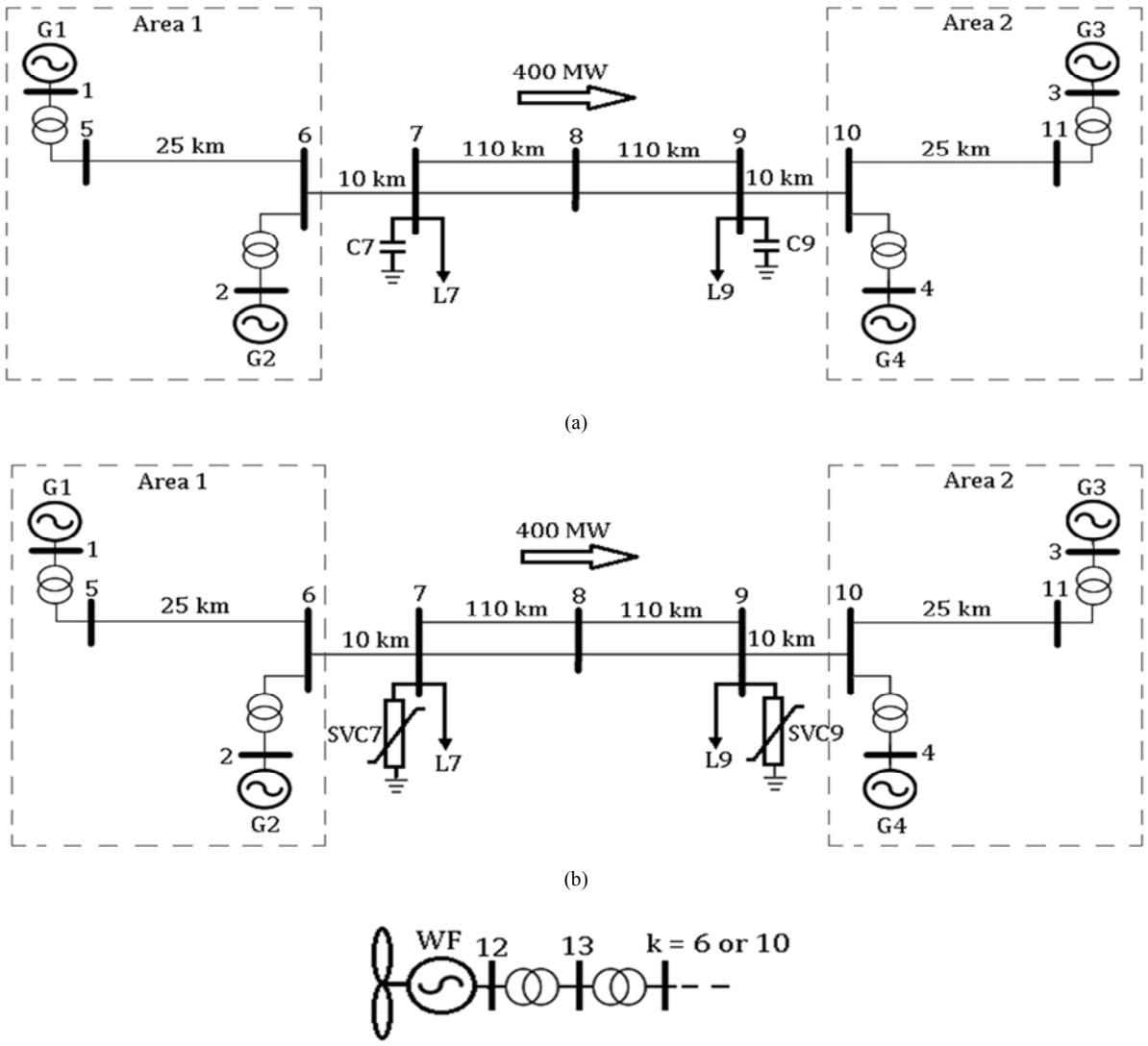

Figure 4. *The study system. (a) Original Kundur's two-area system; (b) Modified system with fixed capacitors replaced by SVCs; (c) Integration of a wind farm at bus k in the Kundur's system.*

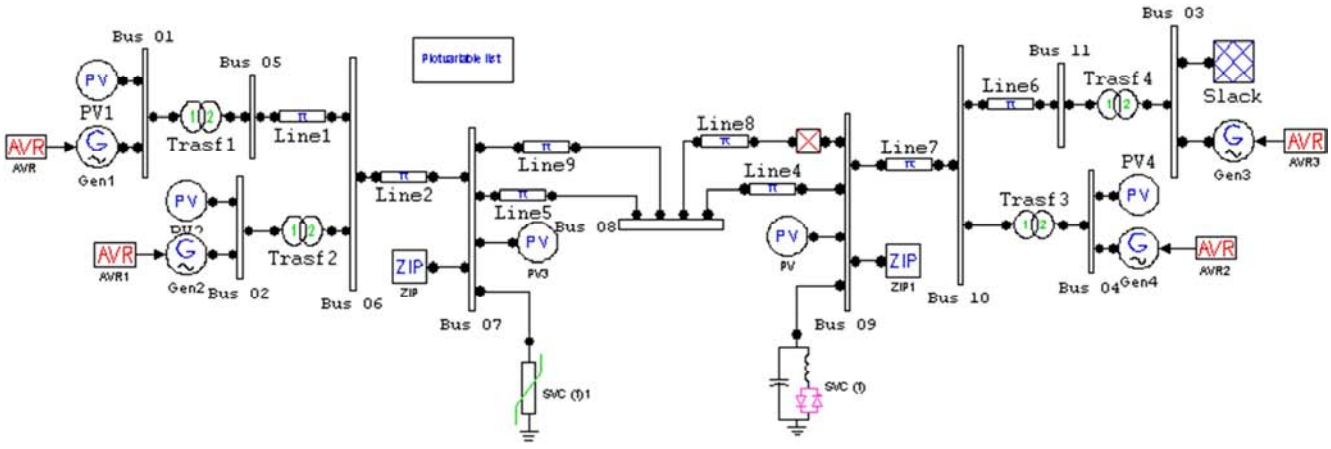

Figure 5. *PSAT model of the system shown in Figure 4(b).*

a) Situation 1: the wind power will be used to replace a specific amount of the conventional generation in area 1. The objectives here are to reduce the ecological impact of the conventional generation and to reduce the dependency on fossil fuels.

b) Situation 2: The wind power will be added to the

conventional generation capacity available in area 2. The main objective in this case is to reduce the dependency of area 2 on area 1 i.e. the minimization of the power transfer over the weak tie-link.

The maximum or allowable amounts of wind power for both scenarios and both situations will be determined based on the modal analysis of the system. In addition, the PODs will be designed by conventional and optimization methods while the wind power is very close to its allowable limits.

4. Results and Discussions

The results will be presented through studying the system described in Figure 4(b) with the model shown in Figure (5) Considering the two stated scenarios in the previous section. The maximum wind penetrations that can be replaced or added to the system are estimated based on the eigenvalue criteria considering SCIG and DFIG technologies. The maximum wind penetration is the maximum value of the wind power after which the system will lose its stability. Two methods can be applied to obtain the maximum wind penetration levels which are the time-domain simulation (TDS) of a specific fault location/duration and eigenvalues analysis. As the TDS is highly dependent on the considered disturbance, the maximum wind penetration level will be determined by the eigenvalues analysis which is independent on the considered disturbances. Near the maximum penetration point, POD will be designed using the frequency response method and the GA method. The target is improving the system dynamic performance when the system is subjected to a small disturbance.

4.1. Scenario 1 with SCIG

Detailed data for the SCIG-based wind turbine and wind model can be found in [36].

(A) Power Replacement

The SCIG will be added to area 1 on bus 12 as shown in Figure 6 for replacing the generated power of the conventional generators by wind power till reaching the maximum wind penetration. The eigenvalues with low damping ratios are listed in Table 1.

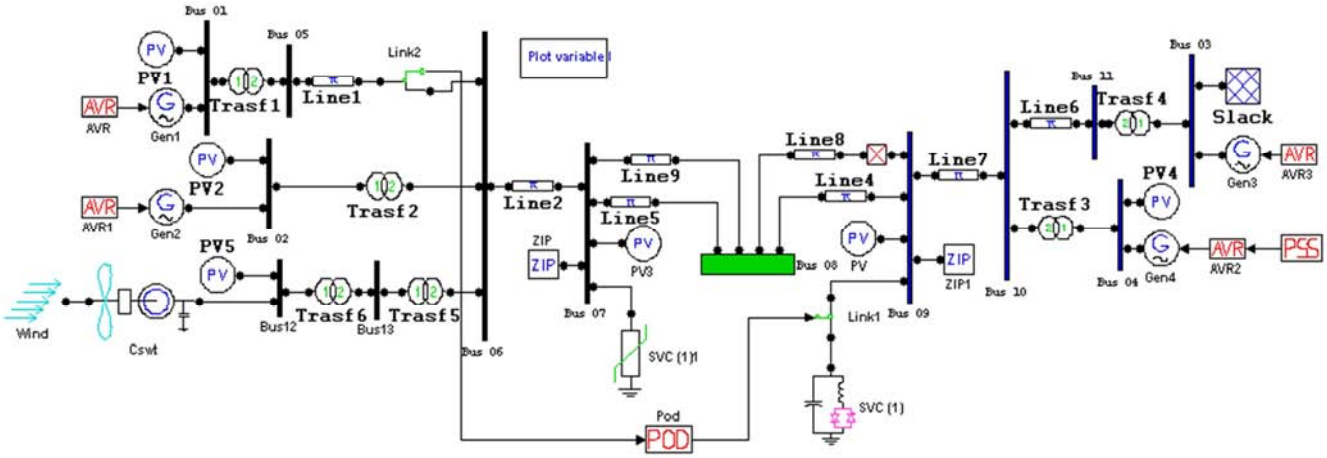

Figure 6. *Two area test system with SCIG added to Area 1.*

Table 1. *Dominant eigenvalues of scenario 1.A.*

	Eigenvalues	f (Hz)	ξ (%)
P_1+P_2=1260MW	-0.59442±j6.5443	1.0458	9.04%
P_{12}=140MW	-0.15025±j3.821	0.6086	3.90%
	-0.57982±j6.5303	1.0434	8.88%
P_1+P_2=1250MW	-0.14699±j3.8239	0.60903	3.86%
P_{12}=150MW	-0.42722±j7.0026	1.1166	6.08%
	0.12483+j0	0	-------

According to the results in Table 1, the maximum generated power in area 1 that can be replaced by wind power equals 140 MW (10% of the total generated power by synchronous generators in Area 1) and after this value the system will be unstable as there is an existence of an eigenvalue located in the unstable region. The POD is then designed using the frequency method near the maximum wind penetration point (P_{12}=140 MW) with the objective of increasing the damping ratios of the eigenvalues to an acceptable level. According to Table 1, at P_{12} = 140 MW, there is a critical eigenvalue with damping ratio 3.9% and an unacceptable eigenvalue with damping ratio 9.04%.

These damping ratios can be increased to acceptable levels (≥10%) by designing a POD. In the first design step of POD, the washout filter time constant is chosen as T_w = 1 [20]. In the next step, the root-locus of all possible stabilizing signals to the POD are determined to select the best signal which can improve the damping ratios of the two eigenvalues shown in Table 1 to an accepted levels. Testing all possible POD stabilizing signals according to its own root-locus leads to finding that the sending current between Bus 5 and Bus 6 as a stabilizing signal to the POD can achieve this target. This reference signal will be considered in all design cases in the paper. The POD gain (K_w) is selected based on the root-locus of the system as shown in Figure 7. It is shown that with a gain of 0.114 the 3.9% damping ratio becomes 23.88% while the 9.04% damping ratio becomes 10.7%. Therefore, this gain value results in acceptable damping ratios.

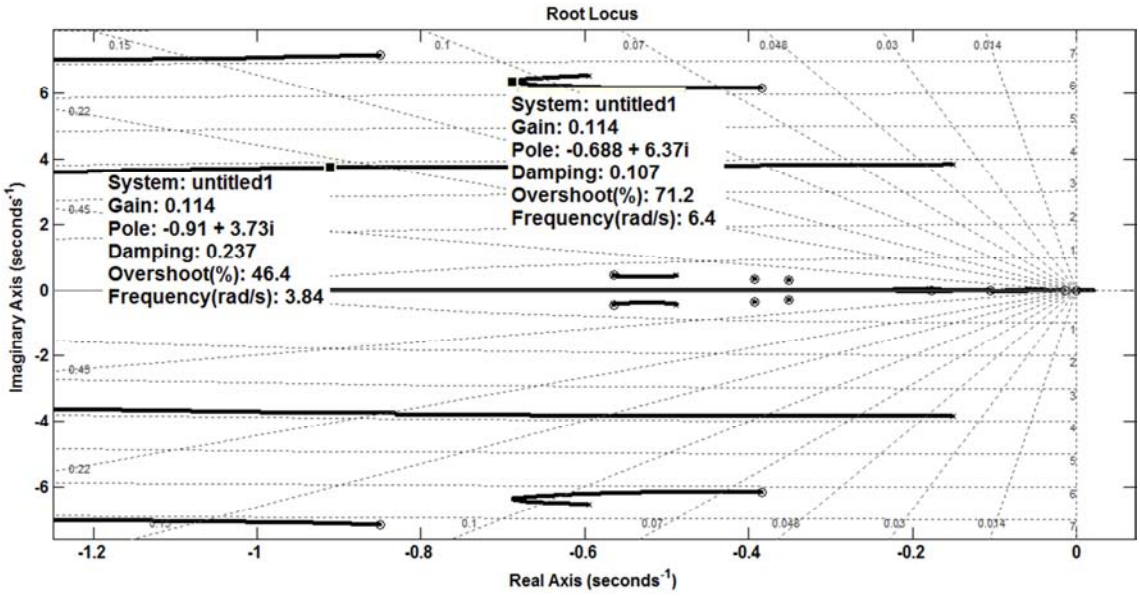

Figure 7. *Root locus of the compensated system and selection of the gain K_w for Scenario 1.A.*

Using the frequency domain POD design method [20, 27], the rest of the POD parameters are determined. The transfer function of the POD is, then takes the form:

$$POD(s) = 0.114\left[\frac{s}{s+1}\right]\left[\frac{0.3186s+1}{0.215s+1}\right]^2 \qquad (14)$$

The POD can be also designed by the GA method using the objective function described in (13). The resulting transfer function takes the form,

$$POD(s) = 0.1545\left[\frac{s}{s+1}\right]\left[\frac{0.2377s+1}{0.2543s+1}\right]^2 \qquad (15)$$

With the POD connected to the system as shown in Figure 6, the design is evaluated by both the eigenvalue analysis and the TDS of the compensated system. The results of the eigenvalue analysis of the compensated system are shown in Table 2 and Table 3 which indicate that the minimum damping ratios of the critical and unacceptable eigenvalues are improved to acceptable levels by the two design methods and this ensures the success of the POD design for improving the damping of the system. The TDS is performed considering a disconnection of line 8 for 100 msec. This disturbance started at t = 1 sec. The responses of the system with and without POD are compared as shown in Figure 8.

Table 2. *Frequency response method based eigenvalues analysis of the compensated system of scenario 1.A.*

Eigenvalues	f (Hz)	ξ (%)
-0.91089±j3.7273	0.61067	23.88%
-0.6877±j6.365	1.0189	10.70%

Table 3. *Genetic algorithm based eigenvalues analysis of the compensated system of scenario 1.A.*

Eigenvalues	f (Hz)	ξ (%)
-0.73982±j6.4751	1.0372	11.34%
-0.83283±j4.0651	0.66041	20.07%

It is depicted from Figure 8 that the POD improves the dynamic performance of the system through increasing the system damping, and decreasing the settling time.

(B) Power Addition

The SCIG in this section is added to area 2 on bus 12 as shown in Figure 9 for reducing the power transfer from area 1 to area 2 by adding generated power by SCIG in area 2 till reaching the maximum wind penetration.

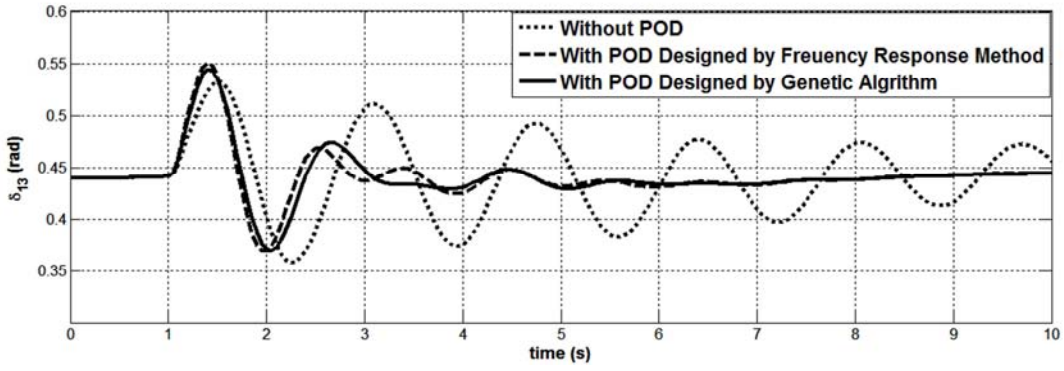

(a)

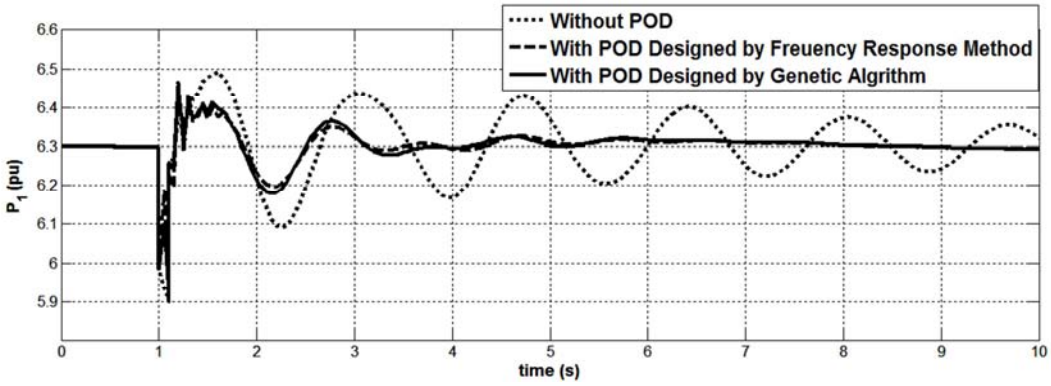

(b)

Figure 8. *TDS for 100msec disconnection of line8: (a) Rotor angle of G1; (b) Active power of G1.*

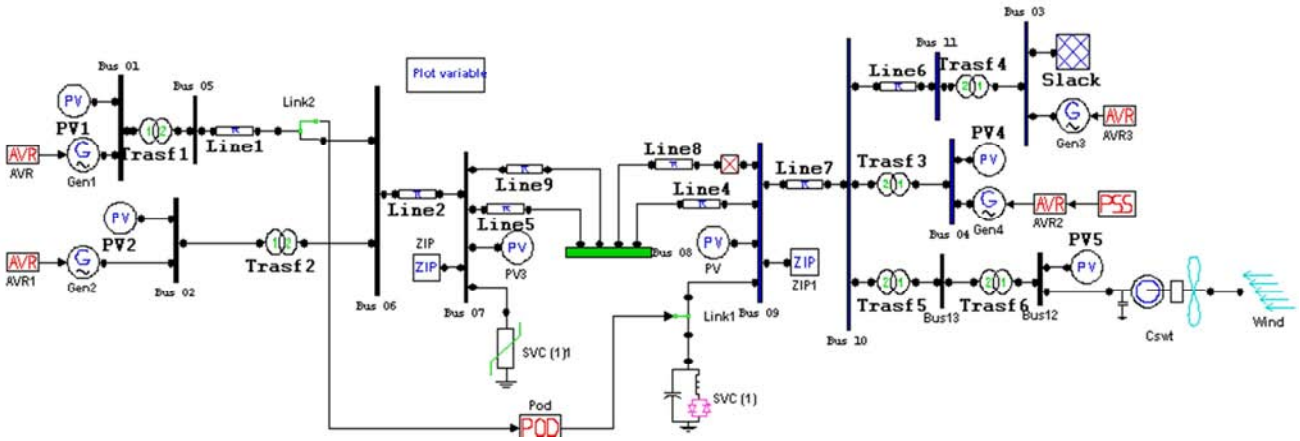

Figure 9. *Two area test system with SCIG added to Area 2.*

The eigenvalues with low damping ratios are shown in Table 4. According to Table 4, the maximum wind power that can be added to area 2 also equals 140 MW and the system will be unstable when the generated power by SCIG equals 150 MW. The POD is designed by the frequency response method near the maximum wind penetration point (P_{12}=140 MW). According to Table 4, at P_{12} = 140 MW, there is a critical eigenvalue with damping ratio 4.31% and an unacceptable eigenvalue with damping ratio 9.02%. The POD gain (K_w) is selected based on the root-locus method. For a gain of 0.062, the 4.31% damping ratio becomes 17.2% while the 9.02% damping ratio becomes 10.16%.

Table 4. *Dominant eigenvalues of Scenario 1.B.*

	Eigenvalues	f (Hz)	ξ (%)
P_{12}=140 MW	-0.59524±j6.5765	1.051	9.02%
	-0.17052±j3.9459	0.6286	4.31%
P_{12}=150 MW	-0.60136±j6.5699	1.05	9%
	-0.16879±j3.9522	0.62958	4.30%
	-0.57935±j6.9841	1.1154	8.28%
	0.17508+j0	0	-------

In this case, the transfer function of the POD will take the form,

$$POD(s) = 0.062\left[\frac{s}{s+1}\right]\left[\frac{0.3097s+1}{0.2074s+1}\right]^2 \qquad (16)$$

With the GA method, the POD transfer function is determined as,

$$POD(s) = 0.0642\left[\frac{s}{s+1}\right]\left[\frac{0.3256s+1}{0.1938+1}\right]^2 \qquad (17)$$

With the POD connected to the system as shown in Figure 9. The results of the eigenvalue analysis of the compensated system are shown in Table 5 and Table 6 which indicate that the minimum damping ratios of the critical and unacceptable eigenvalues are improved to acceptable levels by the two design methods.

Table 5. *Frequency response method based eigenvalues analysis of the compensated system of scenario 1.B.*

Eigenvalues	f (Hz)	ξ (%)
-0.68085±j3.8909	0.62866	17.23%
-0.66545±j6.4604	1.0336	10.16%

Table 6. *Genetic algorithm based eigenvalues analysis of the compensated system of scenario 1.B.*

Eigenvalues	f (Hz)	ξ (%)
-0.87603±j3.6001	0.58969	23.49%
-0.6479±j6.43	1.0181	10%

The responses of the system with and without POD are shown in Figure 10 considering the same disturbance as the previous situation. The results ensure the significant

improvement of the dynamic response of the system with the POD included.

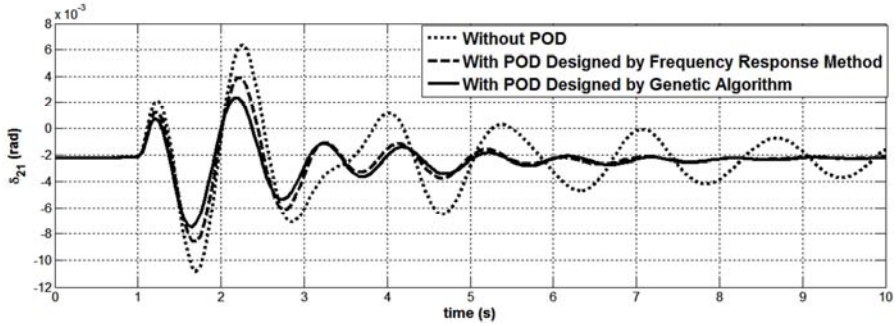

(a)

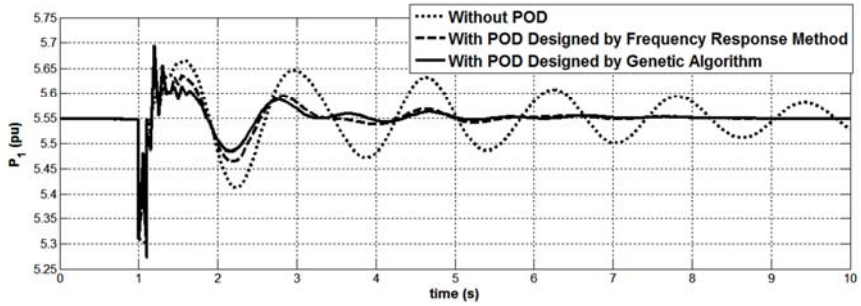

(b)

Figure 10. *TDS for 100msec disconnection of line8: (a) Rotor angle of G2; (b) Active power of G1.*

4.2. Scenario 2 with DFIG

Detailed data for the SCIG-based wind turbine, wind model and collector system can be found in [36]. Detailed analysis of the power replacement and power addition scenarios is provided in the following subsections.

(A) Power Replacement

The DFIG will be added to area 1 for replacing the generated power of synchronous generators by wind power till reaching the maximum wind penetration. The system structure is similar to Figure 6 but the SCIG is replaced with DFIGURE

The eigenvalues with low damping ratios are shown in Table 7. According to Table 7, the maximum generated power in area 1 that can be replaced by wind power equals 500 MW (35.7% of the total generated power by synchronous generators in Area 1).

Table 7. *Dominant eigenvalues of Scenario 2.A.*

	Eigenvalues	f (Hz)	ξ (%)
P_1+P_2=900MW	-0.81087±j6.2776	1.0074	12.80%
P_{12}=500MW	-0.20784±j4.0177	0.64028	5.16%
	-0.85172±j6.2167	0.99866	13.50%
P_1+P_2=850MW	-0.22005±j4.0365	0.64339	5.40%
P_{12}=550MW	-0.12055±j1.7216	0.27467	7.04%
	0.008 ±j0	0	------

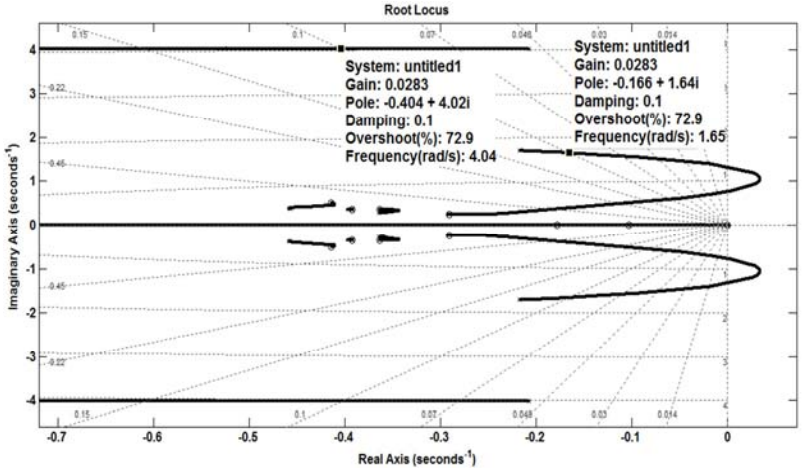

Figure 11. *Root locus of the compensated system and selection of the gain Kw for Scenario 2.A.*

Recalling that the SCIG can offer a maximum power replacement in area 1 by only 10% of the conventional generation, the DFIG offers more than 3.5 times this value. This is attributed to the inherent stability of the DFIG in comparison with the SCIG as well as the grid support that can be provided by the DFIGURE The increased stability associated with the DFIG is provided by its control system (the back-to-back connected converter) which provide reactive power support to the grid and control of active and reactive power outputs. These capabilities are not provided by the SCIG. In addition, SCIG continuously consumes uncontrollable amounts of reactive power which is supplied from the grid considering the partial contribution of the terminal capacitors. Therefore, the SCIG degrades the voltage stability/control of power systems which the DFIG can provide voltage stability/control enhancements. The POD is designed by the frequency response method near the maximum wind penetration point (P_{12}=500 MW). According to Table 7, at P_{12} = 500 MW, there is a critical eigenvalue with damping ratio 5.16%. The POD gain (K_w) is selected based on the root-locus as shown in Figure11. For a gain of 0.0283, the 5.16% damping ratio becomes 10%. The transfer function of the POD takes the form,

$$POD(s) = 0.0283\left[\frac{s}{s+1}\right]\left[\frac{0.2871s+1}{0.2158s+1}\right]^2 \qquad (18)$$

With the GA based design, the POD transfer function becomes,

$$POD(s) = 0.0288\left[\frac{s}{s+1}\right]\left[\frac{0.2874s+1}{0.216+1}\right]^2 9 \qquad (19)$$

The results of the eigenvalue analysis of the compensated system are shown in Table 8 and Table 9 which indicate that the minimum damping ratios of the critical eigenvalues are improved to acceptable level by the two design methods.

Table 8. *Frequency response method based eigenvalues analysis of the compensated system of scenario 2.A.*

Eigenvalues	f (Hz)	ξ (%)
-0.4038±j4.0198	0.643	10%
-0.16551±j1.6452	0.26316	10%

Table 9. *Genetic algorithm based eigenvalues analysis of the compensated system of scenario 2.A.*

Eigenvalues	f (Hz)	ξ (%)
-0.46204±j3.8986	0.62482	11.70%
-0.1687±j1.6572	0.26477	10%

The responses of the system with and without POD are compared as shown in Figure 12 which ensures the effectiveness of the POD in improving the system dynamic stability.

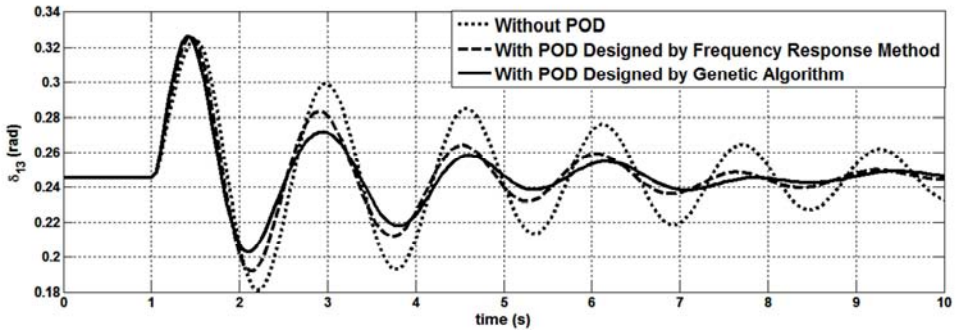

(a)

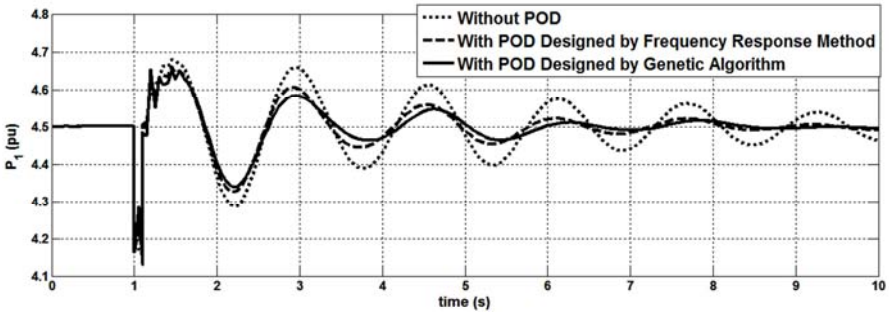

(b)

Figure 12. *TDS for 100msec disconnection of line8: (a) Rotor angle of G1; (b) Active power of G1.*

(B) Power Addition

The DFIG in this section will be added to area 2 (as shown in Figure 9 but the SCIG is replaced with DFIG) for reducing the power transfer from area 1 to area 2 by adding generated power by DFIG in area 2 till reaching the maximum wind penetration. The eigenvalues with low damping ratios are shown in Table 10. According to Table 10, the maximum wind power that can be added to area 2 equals 350 MW. This

value is 2.5 times the maximum amount of SCIG wind power. Again, the DFIG surpasses the SCIG in the power addition. The reasons are also attributed to the control capabilities of the DFIGs in comparison with the SCIGs. It is also shown in Table 10, at P_{12} = 350 MW, there is a critical eigenvalue with damping ratio 6.65%. The POD gain (K_w) is selected based on the root-locus method. For a gain of 0.03, the 6.65% damping ratio becomes 18%. In this case, the transfer function of the POD based on the frequency response method is represented by equation (20) while its form as determined by the GA based method is represented by equation (21).

Table 10. *Dominant eigenvalues of Scenario 2.B.*

	Eigenvalues	f (Hz)	ξ (%)
P_{12}=350 MW	-0.78117±j6.3636	1.0204	12.30%
	-0.27893±j4.182	0.66706	6.65%
P_{12}=400 MW	-0.83732±j6.2965	1.0109	13.06%
	-0.30421±j4.2103	0.67183	7.10%
	-0.22003±j1.3624	0.21964	16.60%
	-0.00074±j0	---------	--------

$$POD(s) = 0.03\left[\frac{s}{s+1}\right]\left[\frac{0.3365s+1}{0.1699s+1}\right]^2 \quad (20)$$

$$POD(s) = 0.034\left[\frac{s}{s+1}\right]\left[\frac{0.3352s+1}{0.1042s+1}\right]^2 \quad (21)$$

The results of the eigenvalue analysis of the compensated system are shown in Table 11 and Table 12 which indicate that the minimum damping ratio of the critical eigenvalue is improved to acceptable level by the two design methods. The responses of the system with and without POD are compared as shown in Figure 13.

Table 11. *Frequency response method based eigenvalues analysis of the compensated system of scenario 2.B.*

Eigenvalues	f (Hz)	ξ (%)
-0.73327±j6.23	0.99838	11.63%
-0.75215±j4.1104	0.66505	18%

Table 12. *Genetic algorithm based eigenvalues analysis of the compensated system of scenario 2.B.*

Eigenvalues	f (Hz)	ξ (%)
-0.84121±j3.7922	0.61822	21.63%
-0.6293±j6.26	1.001	10%

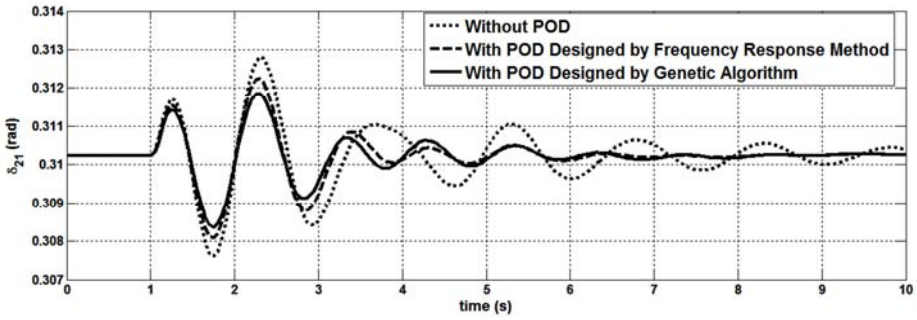

(a)

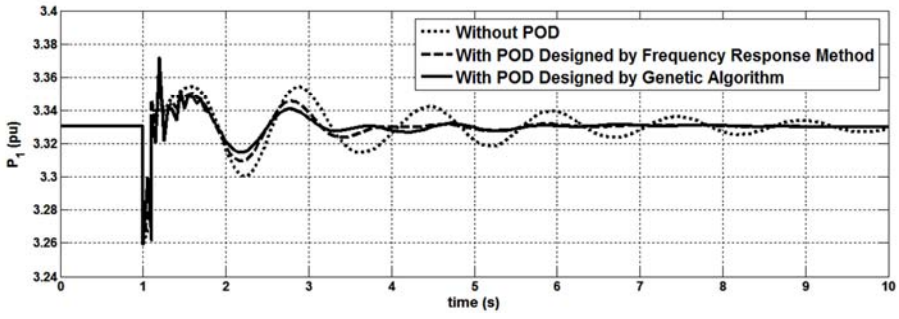

(b)

Figure 13. *TDS for 100msec disconnection of line8: (a) Rotor angle of G2; (b) Active power of G1.*

4.3. Adaptive Controller Parameters Based Genetic Algorithm

In this section, adaptive controller parameters will be obtained based on the genetic algorithm method to enhance the system dynamic stability at different operating points corresponding to different wind penetration levels. The POD will be designed in the two area test system (Figure 4(b)). The two types of WTGs considering the power replacement situations are simulated for some selected operating conditions. The impact on the system dynamic performance is evaluated in a range of operating points. The effectiveness of a POD design under specific operating point for a wide range of operating points is also investigated in this section. The effectiveness indictor is the capability of the POD to

keep the minimum damping ratio of the system at an acceptable level. The results are confirmed by both eigenvalue analysis and time domain simulation in the range of the minimum to maximum wind penetration levels.

(A) Scenario 1 with SCIG

The POD parameters are obtained by GA considering only the maximum wind penetration level (i.e. 140 MW) and it is found that these parameters are effective in the range of the minimum (i.e. 0.0 MW) to maximum penetration levels as shown in Figure 14. The results ensure that the POD has the ability to keep the system eigenvalues in acceptable levels (>=10%) for the entire range of wind power penetration.

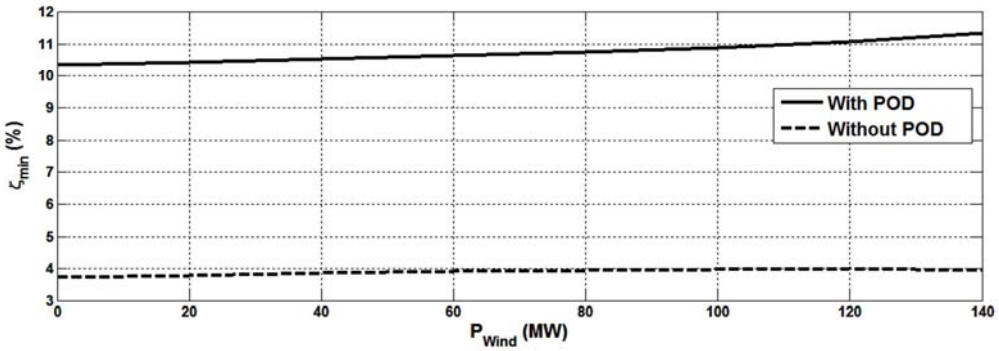

Figure 14. *The minimum damping ratios in case of different wind penetration levels.*

Confirmation of results by eigenvalues analysis and time domain simulation have been demonstrated by taking a random value of the wind penetration level in the wind penetration range (the selected value is 100 MW). The results of the eigenvalue analysis as shown in Table 13. The results of Figure 14 and Table 13 ensure the effectiveness of the POD designed at a specific operating point to a wide range of other operating points.

The results are also confirmed by comparing the system dynamic responses with and without POD as shown in Figure 15 for the same wind power level of 100 MW.

Table 13. *Eigenvalue analysis considering SCIG.*

Eigenvalues	f (Hz)	ξ (%)
Without POD (P_{wind} = 100MW)		
-0.57133±j6.5747	1.0503	8.64%
-0.15157±j3.8125	0.60725	3.94%
With POD (P_{wind} = 100MW)		
- 0.71778±j6.5545	1.0494	10.96%
- 0.83812±j4.0435	0.65723	20.30%

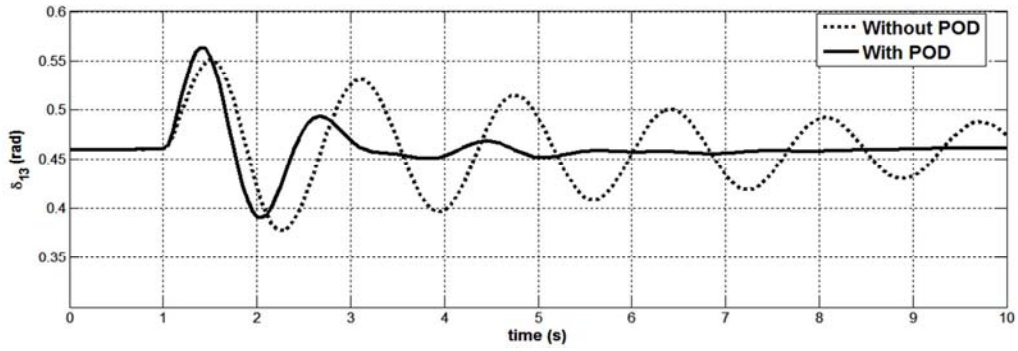

(a)

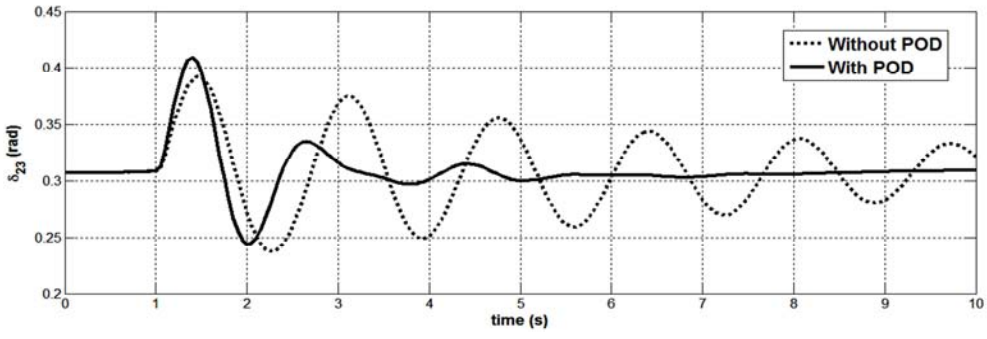

(b)

Figure 15. *TDS for 100msec disconnection of line8: (a) Rotor angle of G1; (b) Rotor angle of G2.*

(B) Scenario 2 with DFIG:

The GA method is applied and it is found that the adaptive POD parameters for various ranges of wind penetration levels as shown in Table 14 and Figure 16 ensures that the POD has the ability to keep the system damping ratios in accepted levels for a wide range of DFIG-based wind power penetration levels.

Table 14. *The effective Range of the POD Parameters of Scenario 2.A.*

Range of P_{wind} (MW)		POD Parameters		
From	To	K_w	T_1	T_2
0	40	0.079	0.661	0.348
50	290	0.07	0.3005	0.2162
300	460	0.034	0.292	0.216
470	500	0.0288	0.2874	0.216

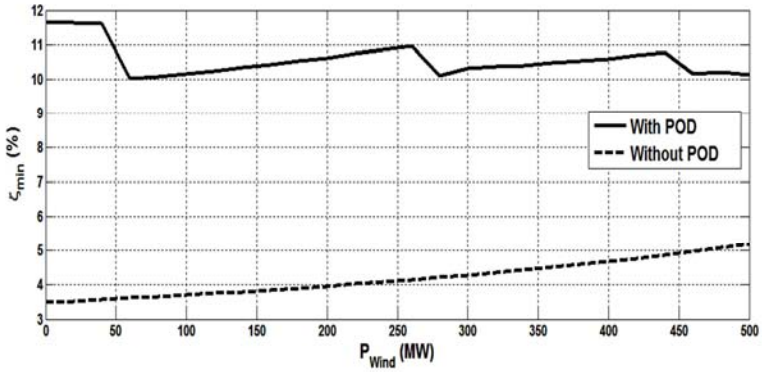

Figure 16. *The minimum damping ratios in case of different wind penetration levels.*

Confirmation of results by eigenvalues analysis and time domain simulation are achieved by taking a random value of the wind penetration in the above ranges (400 MW); the results are in Table 15 and Figure 17. The results of this section ensure the effectiveness of the POD for a wide range of DFIG-based wind penetration levels.

Table 15. *Eigenvalue analysis considering DFIG*

Eigenvalues	f (Hz)	ξ (%)
Without POD (P_{wind} = 400MW)		
-0.73508±j6.3815	1.0224	11.44%
-0.18656±j3.9988	0.63712	4.65%
-0.22921±j1.6007	0.25736	14.22%
With POD (P_{wind} = 400MW)		
- 0.74982±j6.3492	1.0175	11.70%
- 0.42647±j3.9984	0.63998	10.59%
- 0.16858±j1.5439	0.24718	10.61%

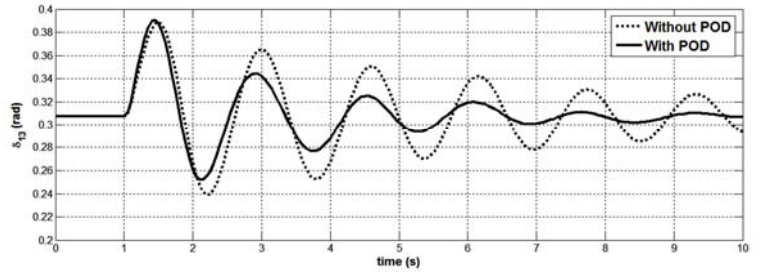

(a)

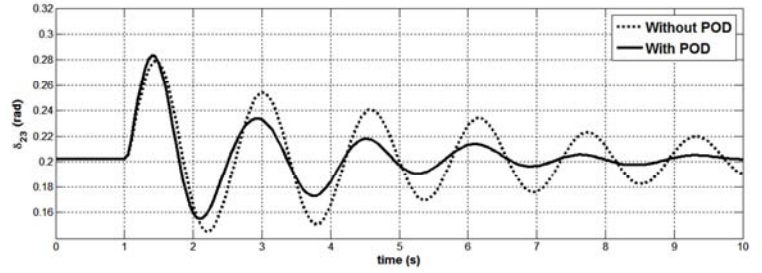

(b)

Figure 17. *TDS for 100msec disconnection of line8: (a) Rotor angle of G1; (b) Rotor angle of G2.*

5. Conclusion

The traditional frequency domain and the GA-based parameter optimization methods for control design are presented in this paper for the design of FACTS-POD controllers. The main objective is the enhancement of the dynamic stability of power systems by keeping a minimum damping ratio of 10%; a value which is acceptable by utility systems. The paper also considers the impact of various wind power technologies on the dynamic stability of power systems. In addition, successful POD designs are presented considering the addition of wind power to conventional generating systems as well as replacement of conventional generating systems by wind power. The maximum wind penetration levels for numerous situations and operating scenarios are estimated based on the eigenvalue stability criterion. With the increase of wind power penetration, it is found that the DFIGs cause less degradation of the system stability in comparison with the SCIGs. In addition, the maximum penetration levels of DFIGs are significantly high in comparison with SCIGs. The control and grid support capability of DFIGs are the main reason of the superiority of DFIGs over SCIGs. The effectiveness of PODs with fixed parameters (determined at a specific operating point) to enhance the system stability over a wide range of operating conditions is carefully investigated. The results show that PODs can provide an effective enhancement of the dynamic stability over a wide range of operating conditions. GA-based adaptive tuning of PODs is also presented in this paper. The capability of PODs for enhancing the dynamic stability is evaluated by the eigenvalue analysis and the time domain simulation.

References

[1] EL-Shimy M. Dynamic Security of Interconnected Electric Power Systems - Volume 2: Dynamics and stability of conventional and renewable energy systems. Lap Lambert Academic Publishing / Omniscriptum Gmbh & Company Kg; Germany; ISBN: 978-3-659-80714-5; Nov. 2015.

[2] Ulbig A, Borsche TS, Andersson G. Impact of low rotational inertia on power system stability and operation. IFAC Proceedings Volumes. 2014 Dec 31;47(3):7290-7.

[3] Shah R, Mithulananthan N, Bansal RC, Ramachandaramurthy VK. A review of key power system stability challenges for large-scale PV integration. Renewable and Sustainable Energy Reviews. 2015 Jan 31;41:1423-36.

[4] El-Shimy M. Viability analysis of PV power plants in Egypt. Renewable Energy. 2009 Oct 31;34(10):2187-96.

[5] Beaudin M, Zareipour H, Schellenberglabe A, Rosehart W. Energy storage for mitigating the variability of renewable electricity sources: An updated review. Energy for Sustainable Development. 2010 Dec 31;14(4):302-14.

[6] EL-Shimy M. Probable power production in optimally matched wind turbine generators. Sustainable Energy Technologies and Assessments. 2013 Jun 30;2:55-66.

[7] EL-Shimy M. Wind Energy Conversion Systems: Reliability Prospective. In Sohail Anwar (ed.) Encyclopedia of Energy Engineering and Technology, Taylor & Francis - CRC Press, 2015.

[8] EL-Shimy M, and Ghaly N. Grid-Connected Wind Energy Conversion Systems: Transient Response. In Sohail Anwar (ed.) Encyclopedia of Energy Engineering and Technology, Taylor & Francis - CRC Press, 2015.

[9] El-Shimy M. Stability-based minimization of load shedding in weakly interconnected systems for real-time applications. International Journal of Electrical Power & Energy Systems. 2015 Sep 30;70:99-107.

[10] EL-Shimy M, Badr MAL, Rassem OM. Impact of Large Scale Wind Power on Power System Stability. MEPCON'08 IEEE International Conference; 12 – 15 March 2008; Aswan, Egypt, 2008. p. 630 – 636.

[11] M. Mandour, M. EL-Shimy, F. Bendary, and W.M.Mansour, "Impact of Wind Power on Power System Stability and Oscillation Damping Controller Design", Industry Academia Collaboration (IAC) Conference, 2015, Energy and sustainable development Track, Apr. 6 – 8, 2015, Cairo, Egypt.

[12] Ghaly N, EL-Shimy M, Abdelhamed M, "Consistence of Wind Power Technologies with the Fault Ride-through Capability Requirements," presented at the MEPCON'14 IEEE International Conference, Cairo, Egypt, 2014.

[13] Chen Z. Issues of connecting wind farms into power systems. InTransmission and Distribution Conference and Exhibition: Asia and Pacific, 2005 IEEE/PES 2005 (pp. 1-6). IEEE.

[14] El-Shimy M. Modeling and analysis of reactive power in grid-connected onshore and offshore DFIG-based wind farms. Wind Energy. 2014 Feb 1;17(2):279-95.

[15] Ahmed M, El-Shimy M, Badr MA. Advanced modeling and analysis of the loading capability limits of doubly-fed induction generators. Sustainable Energy Technologies and Assessments. 2014 Sep 30;7:79-90..

[16] W. Qiao, Harley, R. G. and Venayagamoorthy, G. K., "Effects of FACTS Devices on a Power System Which Includes a Large Wind Farm," presented at the Power Systems Conference and Exposition, 2006. PSCE '06. 2006 IEEE PES, Atlanta, GA, 2006.

[17] EL-Shimy M, Abuel-wafa AR. Implementation and Analysis of Genetic Algorithms (GA) to the Optimal Power Flow (OPF) Problem. Scientific Bulletin - Faculty of Engineering - Ain Shams Uni. 2006; 41(1):753 - 771.

[18] P. Kundur, "Power system stability and control", New York: McGrew Hill, (1994).

[19] T. Ackermann, Wind power in power systems vol. 140. Chichester, UK: John Wiley, 2005.

[20] M. Mandour, M. EL-Shimy, F. Bendary, and W. M. Mansour, "Damping of Power Systems Oscillations using FACTS Power Oscillation Damper – Design and Performance Analysis", MEPCON'14 IEEE International Conference; Dec. 23 – 25, 2014, Cairo, Egypt, 2014.

[21] R. Sadikovic, P. Korba and G. Andersson, "Application of FACTS devices for damping of power system oscillations," presented at the IEEE Power Tech, St. Petersburg, Russia, June 2005

[22] Martins, Nelson, H. J. C. P. Pinto, and John J. Paserba, “Using a TCSC for line power scheduling and system oscillation damping-small signal and transient stability studies,” *Proceedings of IEEE PES Winter Meeting*. Vol. 2. 2000.

[23] F. Milano. PSAT version 2.1.7 Available: http://www3.uclm.es/profesorado/federico.milano/psat.htm.

[24] F. Milano, "An Open Source Power System Analysis Toolbox” IEEE Transactions on Power Systems," IEEE Transactions on Power Systems, vol. 20, Aug 2005.

[25] I. The MathWorks. MATLAB and Simulink R2012a. Available: http://www.mathworks.com

[26] C. E. Ugalde-Loo, et al., "Multi-machine power system state-space modelling for small-signal stability assessments," Applied Mathematical Modelling, vol. 37, pp. 10141-10161, 15 December 2013.

[27] H. M. Ayres, I. Kopcak, M. S. Castro, F. Milano and V. F. d. Costa, "A didactic procedure for designing power oscillation damper of facts devices", Simulation Modelling Practice and Theory, vol.18, no.6 June 2010.

[28] F. Milano, Power System Analysis Toolbox – Documentation for PSAT Version 2.0.0, Feb 2008.

[29] N. Martins and L. Lima, "Eigenvalue and Frequency Domain Analysis of Small-Signal Electromechanical Stability Problems," IEEE Symposium on Application of Eigenanalysis and Frequency Domain Method for System Dynamic Performance, 1989.

[30] B. C. Pal, "Robust pole placement versus root-locus approach in the context of damping interarea oscillations in power systems," IEE Proceedings on Generation, Transmission and Distribution, vol. 149, Nov 2002.

[31] M. EL-Shimy. Dynamic Security of Interconnected Electric Power Systems - Volume 1. Lap Lambert Academic Publishing / Omniscriptum Gmbh & Company Kg; Germany; ISBN: 978-3-659-71372-9; May, 2015.

[32] Passino K. M., "Intelligent Control: An Overview of Techniques," in T. Samad, Ed., Perspectives in Control Engineering: Technologies, Applications, and New Directions, pp. 104-133, IEEE Press, NY, 2001.

[33] Mitchell, Melanie. "Genetic algorithms: an overview." Complexity, Vol. 1, No. 1, 1995, pp. 31-39.

[34] M. EL-Shimy, and A. R. Abuel-wafa, “Implementation and Analysis of Genetic Algorithms (GA) to the Optimal Power Flow (OPF) Problem”, Scientific Bulletin - Faculty of Engineering - Ain Shams University, vol. 41, no. 1, pp. 753 – 71, 2006.

[35] A Aghazade, A. Kazemi, M. M. Alamuti, " Coordination among facts POD and PSS controllers for damping of power system oscillations in large power systems using genetic algorithm," presented at Universities Power Engineering Conference (UPEC), 2010 45th International, Cardiff, Wales, Aug. 31 2010-Sept. 3 2010.

[36] J. C. Munoz and C. A. Canizares, "Comparative stability analysis of DFIG-based wind farms and conventional synchronous generators," presented at the Power Systems Conference and Exposition (PSCE), 2011 IEEE/PES, Phoenix, AZ, 2011.

[37] Mehta B, Bhatt P, Pandya V. Small signal stability analysis of power systems with DFIG based wind power penetration. International Journal of Electrical Power & Energy Systems. 2014 Jun 30;58:64-74.